Journal of Materials Chemistry C

Accepted Manuscript

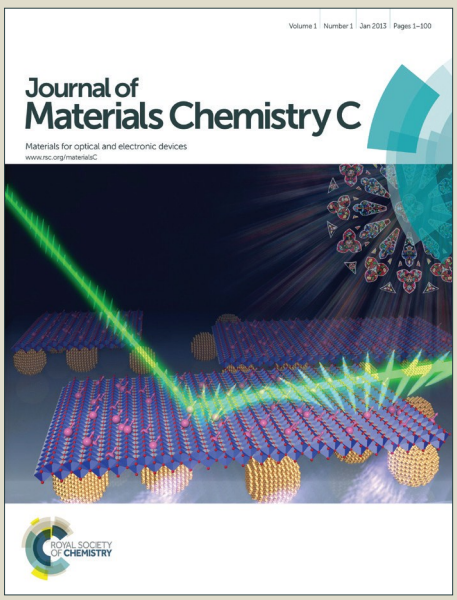

ROYAL SOCIETY OF CHEMISTRY

www.rsc.org/materialsC

Journal of Materials Chemistry C

COMMUNICATION

Improving luminescence performance of quantum dots-based on photonic crystals for white-light-emission

Received 00th January 20xx,
Accepted 00th January 20xx

DOI: 10.1039/x0xx00000x

www.rsc.org/

Heng Li[a], Zhaohua Xu[a,] *, Bin Bao[b], Ning Sun[a]and Yanlin Song[b,] *

A very bright white light is fabricated by combining the advantage of the red, green and blue (RGB) QDs with the photonic crystals (PCs) structure. The results show that the intensity of RGB emission on the PCs can be up to about 8-fold enhancement in comparison to that of the control sample because of the high reflectivity in the UV region by the PCs structure, which possesses a stopband centered at 366 nm to match an excitation source. Furthermore, the chromaticity coordinates of RGB film with the PCs structure remain almost unchanged, close to pure white light. Introducing the PCs into the white light fabrication process has improved not only dispersion of QDs due to large surface-to-volume ratios of inverse opal structure, but also luminous intensity of the white light resulted from effective light-extraction by the PCs. The approach provides a promising strategy for developing the optical device with high performance.

Introduction

Solid state lighting technology combines light emitting diodes (LEDs) offers great promise in meeting the challenge of reducing the energy consumption.[1,2] Bright and efficient white LEDs account for a large proportion of the LEDs market and are rapidly evolving for use in general illumination applications, including automobile headlamps, display backlighting, lamps and fixtures. Apart from increasing the internal quantum efficiencies of LED chips for multiple quantum well sources, improving the performance of luminescent materials for brightness, efficiency and stability, together with packaging into luminaries of high light-extraction efficiency are examples of contemporary challenges. Quantum dots (QDs) are rising as a promising candidate due to their advantageous optical properties, such as good photo-stability, high luminescence efficiency, facile color tenability by the quantum confinement effect.[3,4] Combined with a blue or near-UV LED chip, highly efficient QDs have been used as downconverters, taking advantage of the high excitation efficiency of QDs by blue or near-UV photons.[5-7] Up to now, to enhance the overall performance of white LEDs satisfying the requirements for the practical applications by utilizing QDs as photometrically and electrically down-conversion phosphor, great efforts have been made. In one hand, an efficient surface modification strategy to circumvent oxidation of QD surface and to maintain the excellent light emitting capability of QDs is achieved.[8-11] For example, Jang's team reported that a highly luminescent and photostable quantum dot-silica monolith substance was prepared by preliminary surface exchange of the QDs and base-catalyzed sol-gel condensation of silica.[12] In the other hand, optimized device structure within QDs active layers also offers a suitable approach.[13-17] Recently, Nurmikko et al developed the new nanocomposite luminescent materials by adding an extra process step in the white LED device fabrication, where a targeted GaN layer within an epitaxial thin film structure is made nanoporous (NP-GaN). The hybrid device was demonstrated to include the benefits of enhanced light extraction.[14] Although efforts to fabricate white LEDs with high performances are made, designing a simple and low-cost alternative with better luminescence performance for development of white lighting is still underway.

Herein, a strategy of combining the red, green and blue (RGB) QDs-photonic crystals (PCs) composites and UV LED chips is developed for white LEDs. This approach by introducing the PCs to white-light system is shown to accomplish two things: a) the effective dispersion of QDs in the PCs surface due to large surface-to-volume ratios is the critical factor determining their performance, and more importantly b) enhance the light extraction efficiency by the PCs. As we know, PCs has aroused wide research interests recently in many optical devices due to its special light manipulation property.[18-21] Especially, optical gain in PC science is regarded optical amplification mediated by

[a] Department of Material Technology, Jiangmen Polytechnic, Jiangmen, Guangdong 529090, China. *E-mail: xuzhaohua@iccas.ac.cn
[b] Beijing National Laboratory for Molecular Sciences (BNLMS), Key Laboratory of Green Printing, Key Laboratory of Organic Solids, Institute of Chemistry, Chinese Academy of Sciences, Beijing 100190, China. *E-mail: ylsong@iccas.ac.cn
Electronic Supplementary Information (*ESI*) available: [details of any supplementary information *avail*able should be included here]. See DOI: 10.1039/x0xx00000x

stimulated emission of photons.[22-25] For example, Klimov et al. reported amplified spontaneous emission of semiconductor nanocrystals uniformly coated on opal polystyrene surfaces, which is mainly attributed to the reducing group velocity at the edge of the photonic stopband.[26] Cunningham et al. demonstrated a 108-fold enhancement of fluorescence from quantum dots on the PCs.[27] Significant progress has been reported about highly efficient optical storage, TNT detection and so on, making use of fluorescence-amplifying method based the PCs in our previous work.[28-31] Therefore, the improvement of luminescent signals by the PCs is a powerful tool to develop optical devices with high performance.

In this work, a simple and innovative approach based on the PCs was used to prepare white light with a highly uniform illumination distribution. The white QD-LED, consisting of three types of blue, green, and red QDs-PCs composites on a UV LED chip, is fabricated for the general lighting application, showing a bright luminescence. Furthermore, the PCs film with a stopband centered at 366 nm to match an UV excitation source is designed purposefully. Importantly, a 8-fold increase of RGB emission is achieved simultaneously by the structural engineering and also provides rational understanding on the device operation for the design of high performance white light towards practical realization. Thus, amplification of luminescent signal by introducing the PCs into white-light systems can make a significant impact on the development of new devices.

Experimental

Preparation of the silica sol

A silica sol was prepared through the hydrolysis of tetraethyl orthosilicate (TEOS, 28%) using HCl (37%) and ethanol as the catalyst and the mutual solvent, respectively. The solution was allowed to react for 4 h under stirring at room temperature. The prepared silica sol suspension was transparent.

Fabrication of ordered inverse opals of silica

Monodisperse latex spheres of Poly(St-MMA-AA) were synthesized via our previous method.[32] The resulting latex spheres were used directly without purification. The polydispersity of the latex spheres was about 0.5%, which was detected by ZetaPALS BI-90plus (Brookhaven Instrument). The opal photonic crystal (PC) films were fabricated on glass substrates by a vertical deposition method at invariant temperature (80 ℃) and humidity (80%). After the samples were dry, they were sintered at 85 ℃ for 30 min to increase the stability of the samples.

The silica inverse opals were fabricated by firstly infiltrating SiO_2 sol into the interstice of the as-prepared opal PC template and subsequent calcination to remove the opal template. The main process is as follows: the PC templates were placed vertically, and the SiO_2 sol was dropped on the template and made them fully wetted. Subsequently, the wetted samples were allowed to dry at room temperature for 2 h. Finally, the samples were calcined at 500℃for 6 h to remove the PC template.

Preparation of the QDs based PC film

Three kinds of QDs solution were purchased from Sigma-Aldrich and used without purification. The blue, green, and red QDs solution (10 mg/mL chloroform) (mass ratio of R: G: B is =7:6:3) for CdS, ZnS and ZnSeS, respectively, were added into a 1 mL transparent PMMA/chloroform solution (1g of PMMA mixed with 10 ml of chloroform solution). The QDs based PC films were prepared by spin-coating QDs-PMMA–chloroform solutions with different concentrations onto inverse opal PCs, glass (as control sample with planar structure) and the porous nonperiodic SiO_2 substrates at 1200 rpm for 20 s, respectively.

Fabrication of QDs-based LED devices

In order to make practical devices, QD-doped PMMA based inverse opal PCs were coated on InGaN-based UV LED chips (λpeak = 365 nm). The PMMA-coated QD–PCs plates were diced to a size similar to the LED chip and placed on top of the chip. Here, the performance of the white LEDs is defined mainly by the luminous intensity and International Commission on Illumination (CIE) coordination.

Characterization

The SEM images were obtained with a field-emission SEM (JEOL JSM-4800, Japan), after sputtering the samples with a thin layer of gold. The UV-Vis absorbance spectrum was obtained by an UV-Visible spectrophotometer (UV-2600, Japan). The photoluminescence spectrum was measured by a Hitachi F-4500 fluorescence spectrophotometer. The overall quantum yields were evaluated with a calibtated integrating sphere coated with $BaSO_4$.[33,34] The micro-reflectance spectrum observation of the PCs was carried out by combining a reflected microscope (Olympus MX40, Japan) and a fiber optic UV-Vis spectrometer (Ocean Optic HR 4000, USA). The illuminating light was focused onto the PC through an objective lens and the reflected light was collected by the same lens and then transported to the spectrometer through the optic fiber. The large-scaled fluorescent images were taken by a fluorescence scanner (ChampChemi Professional+, China) with 365 nm UV light excitation.

Results and discussion

The three-component QDs mixtures are employed in this work to yield efficient luminescence in the red, green and blue under a single UV light excitation, respectively. At the first, UV-Visible absorption and photoluminescence (PL) spectroscopy of the trichromatic QDs in chloroform solution used here are presented in Fig. 1a, b. The trend of the absorption toward longer wavelength is observed. The PL spectra of the three samples exhibited band-to-band

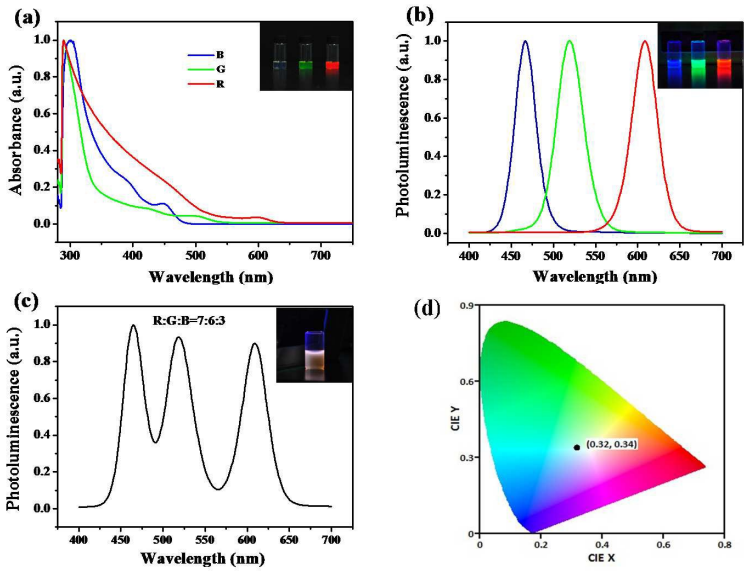

Fig.1 (a) UV-visible absorption and (b) PL spectroscopy of the trichromatic QDs in chloroform solution under excitation wavelength of 365 nm. The inset of (a) shows photographic images of trichromatic QDs, respectively and the emission under UV light for each sample. (c) PL spectrum of trichromatic QDs solution mixture. Inset: photographic image of trichromatic QDs mixture emission under UV light. (d) The CIE coordinates of the emitting trichromatic QDs.

emission centered at 467 nm, 520 nm and 610 nm, respectively. These PL spectra correlate well with the observed RGB emission as shown in the inset Fig. 1b. Their respective PL spectra show large Stokes shifts, indicating that the emission can be dominated by defect-related mechanisms.[35] It could be seen that their full width at half maximums are about 30 nm, indicating their narrow size distribution. An example of a trichromatic QDs mixture is shown in Fig. 1c. The amounts of each of QDs constituent are controlled to achieve equal RGB emission intensities, demonstrating a simple and effective method of fine color rendering capability for illumination devices. The intensities in each of the RGB spectrum regions were almost equal, producing the bright white color shown as a color photographic image in Fig.1c inset. From analyzing the emission spectrum, the Commission Internationale de l'Eclairage (CIE) chromaticity coordinates for the white QD emission yield values of x = 0.32 and y = 0.34 lay in the white light region.

Silica inverse opal PC is fabricated by a sacrificial polymer template method, which involvs the self-assembly of polymer colloidal spheres, infiltration of silica sol and removal of polymer spheres.[36] Topographical character of the P(St-MMA-AA) opal templates and corresponding SiO_2 inverse opals is investigated by scanning electron microscopy (SEM) in Fig. 2a, b. Fig. 2a shows images of P(St-MMA-AA) opal templates with diameters of 260 nm which illustrates the colloid spheres are in a face-centered cubic arrangement with a close-packed plane (111) oriented parallel to the substrate.

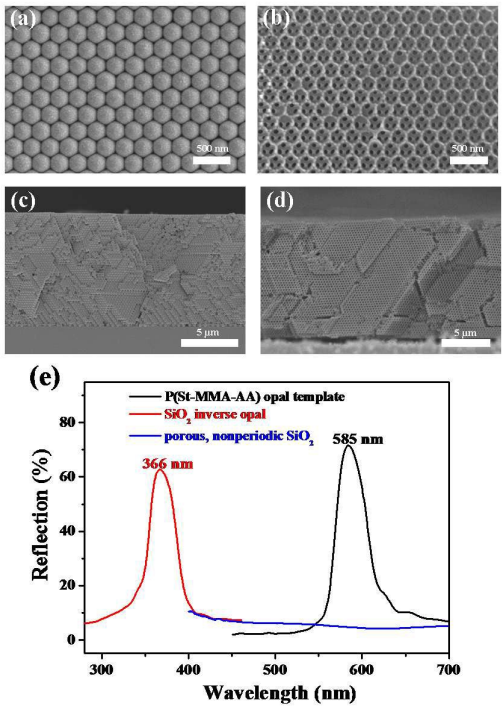

Fig.2 SEM images of P(St-MMA-AA) opal templates with diameters of (a) 260 nm and the corresponding SiO_2 inverse opals with macropore diameters of (b) 210 nm. (c, d) Typical SEM images of cross-section of the P(St-MMA-AA) opal templates and corresponding SiO_2 inverse opals. (e) The reflection spectra for P(St-MMA-AA) opal templates, the corresponding SiO_2 inverse opals and the porous nonperiodic SiO_2 material.

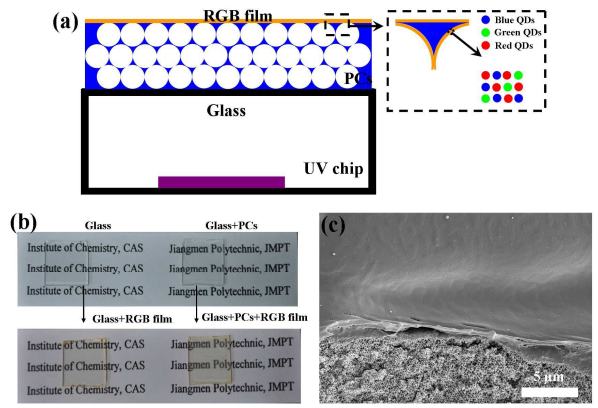

Fig.3 (a) Schematic diagram of a white LED with a mixture of blue, green and red QDs embedded in PMMA matrix on the PCs film on top of a UV-chip. (b) Photographic images of the glass (control sample) and glass coated PC film surfaces (the pixel size of 1 cm × 1 cm^2). The PC film is nearly transparent and become yellowish after spin-coating RGB QDs-PMMA mixture solution. The left panel is coated with the RGB QDs film and the right panel is coated with the film of RGB QDs-PCs composites, respectively. (c) The typical SEM image of cross-section of SiO2 inverse opals coated RGB QDs film.

The close-packed arrangement can extend over a large area, which provides a simple and cheap method for application of white LED devices. The corresponding SiO_2 inverse opals with macropore diameters of 210 nm is showed in Fig. 2b, which are about 80% of the original colloidal sphere due to the shrinkage of polymer spheres. Clearly, latex spheres were well-orderly arranged in the as-prepared opal PC films, which contributed to the well-ordered periodicity of inverse opal PCs. It also shows that the three dark regions inside each hollow region correspond to one air spheres of the underlying layer, indicating the formation of two layers of closely packed cavities. The large hole size of air spheres is beneficial to dispersion of QDs. A cross-section SEM image of the inverse opals is showed in Fig. 1d. Each facet of the PC film shows well-ordered structure over large area, which ensures the excellent optical property of PCs, as will contribute to the amplitude of QDs emission. Additionally, the porous nonperiodic SiO_2 material is obtained as well (Fig. S1 in supporting information), the sample will serve as reference sample to determine the enrichment effect from large surface areas. Fig. 2e exhibits the reflection spectra for P(St-MMA-AA) opal templates and the corresponding SiO_2 inverse opals, indicating the excellent stopband reflectance of the as-prepared PC films. Obviously, after removal of polymer spheres by calcination, the stopband of SiO_2 inverse opals shifts to higher energies remarkably compared with the stopbands of bare opals, which is due to a lower average refractive index caused by air spheres instead of polymer spheres and shrinkage of spheres diameter during calcination. The SiO_2 inverse opal films with good optic properties are important for the modification of light propagation and emission property of QDs. It is noteworthy that microspheres with suitable diameter should be selected to assemble into PCs with given photonic bandgap for the aim of improving QD's emission. Here SiO_2 inverse opals with macropore diameters of 210 nm were fabricated, which is with photonic bandgap just overlapped the UV excitation light. It is also found that the porous nonperiodic SiO_2 material as the reference sample has poor optic properties, which can judge the special light manipulation property of matched PCs.

To combine the advantage of the QDs and the PCs structure, we tried to fabricate a white LED with structure as Fig.3a. A homogeneous mixture of blue, green, and red emissive QDs were dispersed in a PMMA matrix, which was chosen as the matrix polymer because it is relatively transparent over the whole visible spectrum and has reasonable mechanical strength. There has even been a report that the luminescent properties of the QD layers are improved if the QDs are properly embedded in an optically transparent polymer matrix.[37] The QDs-PMMA film is coated on the PCs with a UV-chip providing a 365nm excitation light

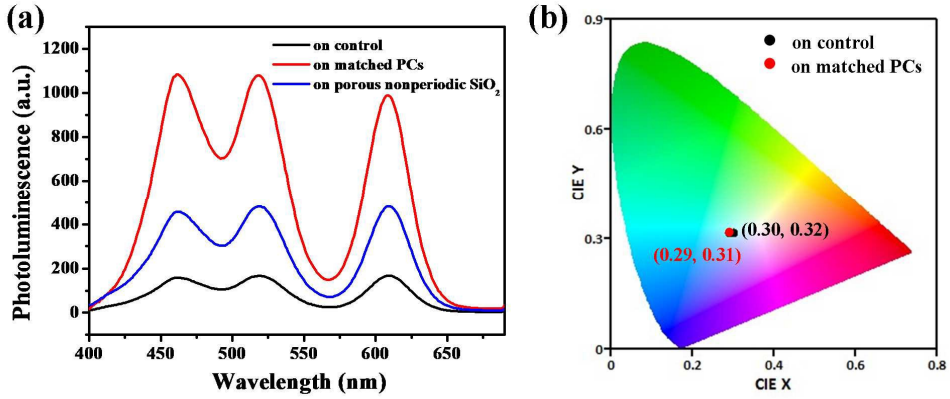

Fig.4 (a) PL spectra and (b) The CIE coordinates of a mixture of blue, green and red QDs embedded in PMMA matrix on the control, on the matched PCs film and the porous nonperiodic SiO_2 under excitation wavelength of 365 nm, respectively.

Table 1 Luminecescence properties of the white-light-emission films on different substrates

Substrate	CIE (X, Y)	Quantum efficiency (%)
Control (glass)	(0.30, 0.32)	14
Porous nonperiodic SiO_2	(0.31, 0.32)	38
Matched PCs	(0.29, 0.31)	60

source to fabricate a white LED. The PC film is nearly transparent and become yellowish after spin-coating RGB QDs-PMMA mixture solution in Fig. 3b, indicating having no interference with white light. Additionally, the thickness of PMMA film loaded QDs can be readily controllable by varying the PMMA and QDs concentration in the mixture solution. Fig. 3c presents a typical SEM image of cross-section of SiO_2 inverse opals coated RGB QDs film with a uniform thickness of ~1 μm.

As shown in Fig. 4a, owing to the tricolor mixing with a suitable ratio, white light emission is satisfactorily achieved. Remarkably, a white-light emission film on the control sample with CIE coordinates of (0.30, 0.32) is obtained and is very close to the pure white light (0.33, 0.33). The PL spectrum of this white-light emissive film shows three distinct emission bands, which correlate well with the emissions of pure films. This observation demonstrates that there is no significant interaction between the three QDs when they are doped in the matrix. However, quantum efficiency of the control sample is only 14% due to the most photon emission restricted by planar surface. In contrast to the results from the QDs emission under a single excite source, the peak wavelength position remained almost unchanged, but the emission intensity from the matched PCs is significantly stronger than that from control sample. Detailedly, about 3-fold emission enhancement occurs to the porous nonperiodic SiO_2 substrate, when comparing with that of the control sample. By the SEM (in Surpporting Information), it is clearly seen that porous nonperiodic SiO_2 have 3D channel structures with large surface, while the control sample has a planar surface. Therefore, this enhancement is mainly resulted from enrichment effect from large surface areas.[29] It is greatly exciting that a 8-fold enhancement is observed for the matched PCs film compared to the control sample, confirming the light-extraction enhancement of PCs. The amplification of emission can be attributed to the combination action of macroporous structure and its periodic arrangement, especially, its periodically modulated structure interacts with excited light. The external excitation of the leaky modes leads to the formation of high-intensity near fields that serve to efficiently excite more red, green and blue QDs.[38,39] More important, quantum efficiency of the matched PCs film can be up to about 60%. In addition, the color coordinates of white emission on the matched PCs shifted slightly from (0.30, 0.32) to (0.29, 0.31), which is still laid in the white light region.

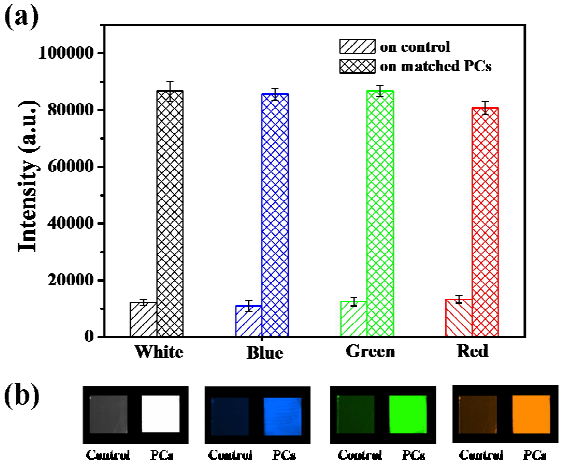

Fig.5 (a) PL intensity and (b) photographic images from left to right show white, blue, green and red colors under UV irradiation.

In order to further evaluate the spectral distribution of ternary QDs, luminescence intensities of single color are measured. The red, green and blue spectral components are collected by the filter installed in the fluorescence scanner, respectively. The enhancements of each spectral component from the PCs over the control sample are shown in Fig. 5a. The enhancement ratio is observed among red, green and blue QD emissions, which is in good accordance with PL emission spectra (Fig. 4a). Moreover, photographic images of RGB spectral component (the pixel size of 1.0 × 1.0 cm^2) in Fig.5b show that device structure can be applicable to large-sized applications. The films show a homogeneous RGB color with strong brightness. It is clearly seen that the images on the matched PCs exhibit higher brightness compared with that on the control, indicating that the PCs does amplify luminescent intensity effectively to attain high brightness. By evaluating the relative intensity, the intensity on the PCs is evidently enhanced, which corresponds to high brightness of the PC surface. Therefore, amplification of luminescent intensity on the PCs presents a feasible strategy for improving brightness of white light.

Conclusions

In summary, we have presented very bright white light enabled by the combination of RGB QDs and the PC structure. The experimental results show that the intensity of RGB emission exhibited considerable enhancement because of the high reflectivity in the UV region by the PCs structure, which possesses a stopband centered at 366 nm to match an excitation source. Introducing the PCs into the white light fabrication process has improved not only dispersion of QDs

but also luminous intensity of the white light. The approaches and results in the present study represent remarkable progress in the device performances of white LEDs and also provide reasonable guidelines for the practicable realization of the high performance white LEDs.

Acknowledgements

This work is supported by the National Natural Science Foundation of China (Grant No. 51302107), the Natural Science Foundation of Guangdong Province, China (Grant No. 2015A030313804) and Training Special Funds of College Students' Innovation of Science and Technology of Guangdong Province, China (Grant No. pdjh2015a0812).

Notes and references

1 C. J. Humphreys, *MRS Bull.*, 2008, **33**, 459.
2 E. F. Schubert and J. K. Kim, *Science*, 2005, **308**, 1274.
3 X. Q. Li, Y. W. Wu, D. Steel, D. Gammon, T. H. Stievater, D. S. Katzer, D. Park, C. Piermarocchi and L. J. Sham, *Science*, 2003, **301**, 809.
4 J. Y. Kim, O. Voznyy, D. Zhitomirsky and E. H. Sargent, *Adv. Mater.*, 2013, **25**, 4986.
5 Y. Shirasaki, G. J. Supran, M. G. Bawendi and V. Bulović, *Nat. photonics*, 2013, **7**, 13.
6 S. Kim, S. HyukIm and S.-W. Kim, Nanoscale, 2013, 5, 5205.
7 K.-S. Cho, E. K. Lee, W.-J. Joo, E. Jan, T.-H. Kim, S. J. Lee, S.-J. Kwon, J. Y. Han, B.-K. Kim, B. L. Choi and J. M. Kim, *Nat. Photonics*, 2009, **3**, 341.
8 C. Yoon, H.-G. Hong, H. C. Kim, D. Hwang, D. C. Lee, C.-K. Kim, Y.-J. Kim and K. Lee, *Colloid Surf. A-Physicochem. Eng. Asp.*, 2013, **428**, 86.
9 P. Tao, Y. Li, R. W. Siegel and L. S. Schadler, *J. Mater. Chem. C,* 2013, **1**, 86.
10 J. Ziegler, S. Xu, E. Kucur, F. Meister, M. Batentschuk, F. Gindele and T. Nann, *Adv. Mater.*, 2008, **20**, 4068.
11 P. Yang, H.-S. Chen, J. P. Wang, Q. Che, Q. Ma, Y. Q. Cao and Y. N. Zhu, *RSC Adv.*, 2014, **4**, 20358.
12 S. Jun, J. Lee, and E. Jang, *ACS Nano*, 2013, **7**, 1472.
13 C. Sun, Y. Zhang, Y. Wang, W. Y. Liu, S. Kalytchuk, S. V. Kershaw, T. Q. Zhang, X. Y. Zhang, J. Zhao, W. W. Yu and A. L. Rogach, *Appl. Phys. Lett.*, 2014, **104**, 261106.
14 C. Dang, J. Lee, Y. Zhang, J. Han, C. Breen, J. S. Steckel, S. Coe-Sullivan and A. Nurmikko, *Adv. Mater.*, 2012, **24**, 5915.
15 X. X. Fu, X. N. Kang, B. Zhang, C. Xiong, X. Z. Jiang, D. S. Xu, W. M. Du and G. Y. Zhang, *J. Mater. Chem.*, 2011, **21**, 9576.
16 B. X. Zhao, D. L. Zhang, K. Sun, X. B. Wang, R. H. Mao and W. W. Li, *RSC Adv.*, 2014, **4**, 45155.
17 K.-J. Chen, H.-C. Chen, K.-A. Tsai, C.-C. Lin, H.-H. Tsai, S.-H. Chien, B.-S. Cheng, Y.-J. Hsu, M.-H. Shih, C.-H. Tsai, H.-H. Shih and H.-C. Kuo, *Adv. Funct. Mater.*, 2012 , **22**, 5138.
18 P. Lodahl, A. F. van Driel, I. S. Nikolaev, A. Irman, K. Overgaag, D. L. Vanmaekelbergh and W. L. Vos, *Nature*, 2004, **430**, 654.
19 J. P. Ge, Y. X. Hu and Y. D. Yin, *Chem. Int. Ed.*, 2007, **46**, 7428.
20 A. C. Arsenault, D. P. Puzzo, I. Manners and G. A. Ozin, *Nat. Photonics*, 2007, **1**, 468.
21 F. Jin, Y. Song, X. Z. Dong, W. Q. Chen and X. M. Duan, *Appl. Phys. Lett.*, 2007, **91**, 031109.
22 J. Han, H. L. Su, D. Zhang, J. J. Chen and Z. X. Chen, *J. Mater. Chem.*, 2009, **19**, 8741.
23 M. N. Shkunov, Z. V. Vardeny, M. C. DeLong, R. C. Polson, A. A. Zakhidov and R. H. Baughman, *Adv. Funct. Mater.*, 2002, **12**, 21.
24 H. J. Kim, S. Kim, H. Jeon, J. Ma, S. H. Choi, S. Lee, C. Ko and W. Park, *Sensors and Actuators B-Chemical*, 2007, **124**, 147.
25 F. Jin, L. T. Shi, M. L. Zheng, X. Z. Dong, S. Chen, Z. S. Zhao and X. M. Duan, *J. Phys. Chem. C.*, 2013, **117**, 9463.
26 G. R. Maskaly, M. A. Petruska, J. Nanda, I. V. Bezel, R. D. Schaller, H. Htoon, J. M. Pietryga and V.I. Klimov, *Adv. Mater.*, 2006, **18**, 343.
27 N. Ganesh, W. Zhang, P. C. Mathias, E. Chow, Jant Soares, V. Malyarchuk, A. D. Smith and B. T. Cunningham, *Nature Nanotechnology,* 2007, **2**, 515.
28 Y. Q. Zhang, J. X. Wang, Z. Y. Ji, W. P. Hu, L. Jiang, Y. L. Song and D. B. Zhu, *J. Mater. Chem.*, 2007, **17**, 90.
29 H. Li, J. X. Wang, Z. L. Pan, L. Y. Cui, L. Xu, R. M. Wang, Y. L. Song and L. Jiang, *J. Mater. Chem.*, 2011, **21**, 1730.
30 H. Li, J. X. Wang, H. Lin, L. Xu, W. Xu, R. M. Wang, Y. L. Song and D. B. Zhu, *Adv. Mater.*, 2010, **22**, 1237.
31 B. Bao, M. Z. Li, Y. Li, J. K. Jiang, Z. K. Gu, X. Y. Zhang, L. Jiang and Y. L. Song, *Small*, 2015, **11**, 1649.
32 J. X. Wang, Y. Q. Wen, H. L. Ge, Z. W. Sun, Y. M. Zheng, Y. L. Song and L. Jiang, *Macromol. Chem. Phys.*, 2006, **207**, 596.
33 J. C. de Mello, H. F. Wittmann and R. H. Friend, *Adv. Mater.*, 1997, **9**, 230.
34 Y. S. Zhu, W. Xu, H. Z. Zhang, W. Wang, S. Xu and H. W. Song, *J. Phys. Chem. C*, 2012, **116**, 2297.
35 W. Liu, Y. Zhang, W. Zhai, Y. Wang, T. Zhang, P. Gu, H. Chu, H. Zhang, T. Cui, Y. Wang, J. Zhao and W. W. Yu, *J. Phys. Chem. C*, 2013, **117**, 19288.
36 Y. Q. Zhang, J. X. Wang, X. Chen, L. Jiang, Y. L. Song and D. B. Zhu, *Appl. Phys. A*, 2007, **87**, 271.
37 M. Böberl, M. V. Kovalenko, S. Gamerith, J. W. List and W. Heiss, *Adv. Mater.*, 2007, **19**, 3574.
38 J. I. L. Chen, E. Loso, N. Ebrahim and G. A. Ozin, *J. Am. Chem. Soc.*, 2008, **130**, 5420.
39 A. Mihi, F. J. Lopez-Alcaraz and H. Miguez, *Appl. Phys. Lett.*, 2006, **88**, 193110.

Table of Contents Image

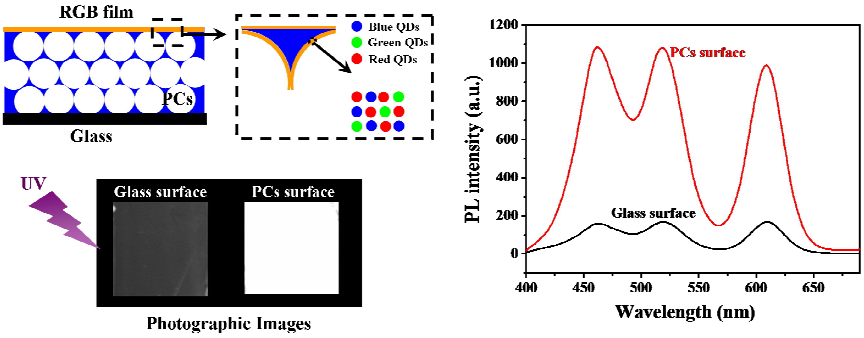

A very bright white light was obtained by combining the advantage of the red, green and blue quantum dots with the photonic crystals structure.

Keywords: Quantum dots, photonic crystals, white light, light extraction.